Low-cost, solution processable carbon nanotube nanocomposite supercapacitors and their characterization

Suvi Lehtimäki[a,], Sampo Tuukkanen[a], Juho Pörhönen[a], Pasi Moilanen[b], Jorma Virtanen[c], Mari Honkanen[d], Donald Lupo[a]

[a] *Tampere University of Technology, Department of Electronics and Communications Engineering, Korkeakoulunkatu 3, FI-33720, Tampere, Finland*
[b] *Morphona Ltd., Myllärintie 1, 40640 Jyväskylä, Finland*
[c] *The University of Akron, Department of Polymer Engineering, 250 South Forge Street, Akron, OH 44325-0301, USA*
[d] *Tampere University of Technology, Department of Materials Science, Korkeakoulunkatu 6, FI-33720, Tampere, Finland*

Abstract

We report ecological and low-cost carbon nanotube (CNT) supercapacitors fabricated using a scalable, one-step solution processing method, where the use of a highly porous and electrically conductive active material eliminates the need for a current collector. Electrodes were fabricated on a poly(ethylene terephthalate) substrate from a printable CNT ink, where the CNTs are solubilized in water using xylan as a dispersion agent. The dispersion method facilitates a very high concentration of CNTs in the ink. Supercapacitors were assembled using a paper separator and an aqueous NaCl electrolyte. Devices were characterized with a galvanostatic discharge method defined by an industrial standard. The capacitance of the 2 cm^2 devices was 12 mF and equivalent series resistance 80 Ω. Low-cost supercapacitors fabricated from safe and environmentally friendly materials have potential applications as energy storage devices in ubiquitous and autonomous intelligence as well as in disposable low-end products.

1. Introduction

Supercapacitors, also called ultracapacitors or electric double layer capacitors (EDLC), have attracted much attention in the last few years due to their potential as efficient, long-life and high-power energy storage devices [1, 2, 3, 4]. Supercapacitors can be fabricated from low-cost, non-toxic and disposable materials, making them an attractive alternative to batteries in e.g. distributed sensor networks and other ubiquitous electronics [5, 6, 7]. Harvesting energy from ambient light, RF fields or vibrations facilitates a long-life, autonomous system, where the supercapacitor can act as an interim energy storage when the primary source is not available [8, 9].

The high surface area materials commonly used in supercapacitors such as activated carbons are poor conductors, leading to a need for conductive additives and metallic current collectors. Carbon nanotubes (CNT) have the advantage of a high surface area in addition to high electrical conductivity [10]. This allows the fabrication of electrodes in a one-step process without a current collector [11]. However, preparation of stable CNT dispersions is very challenging, and the dispersibilities are usually low [12].

Here we present CNT supercapacitors prepared from a composite ink, where the multi-walled nanotubes (MWNT) are dispersed in high concentration (3.5 wt-%) using the polymer xylan, which is a type of hemicellulose. Previously, CNT electrodes have been prepared from dispersions with only 0.1–0.5 wt-% CNTs [6, 13, 14, 15]. In addition to forming a stable, concentrated dispersion of MWNTs, the hemicellulose also improves the printability of the ink by increasing its viscosity, which facilitates mass production. The electrolyte of the supercapacitor is aqueous NaCl, making the entire device easily disposable and safe to use in any environment.

There have been efforts to standardize measurement procedures in supercapacitor electrode material research [16]. Here, an industrial standard [17] is adopted, as the objective is not only to characterize the CNT electrode material, but also to explore the properties of the whole device. The choice of standard device class is also examined via a simple modeling test to determine its the effect on the results.

2. Experimental

Electrodes were fabricated on poly(ethylene terephthalate) (PET) (Melinex ST506 from DuPont) with a carbon nanotube/xylan nanocomposite ink. The ink was manufactured by Morphona Ltd., which is using a patent-pending method where carbon nanotubes are suspended in aqueous solution by using xylan in its acidic form as a dispersion agent. The MWNT (NC7000 from Nanocyl, average diameter 9.5 nm) content of the ink was 3.5 wt-% and the xylan content 1.75 wt-%. The mixing was done by ultrasonication: a typical sonication time for 100 ml was 10 min with 100 W power.

The ink was characterized with field-emission scanning electron microscope (FESEM, Zeiss ULTRAplus) and transmission electron microscope (TEM, Jeol JEM-2010) equipped with energy dispersive x-ray spectrometer (EDS, Noran Vantage with Si(Li) detector, Thermo Scientific). For FESEM studies a drop of the ink was placed on the aluminum pin stub and for TEM studies a drop of the ink was placed on the copper grid with a holey carbon support film. Before microscopy studies, the ink was let to dry at least 24 hours. In addition, the cross-section

Email address: suvi.lehtimaki@tut.fi (Suvi Lehtimäki)

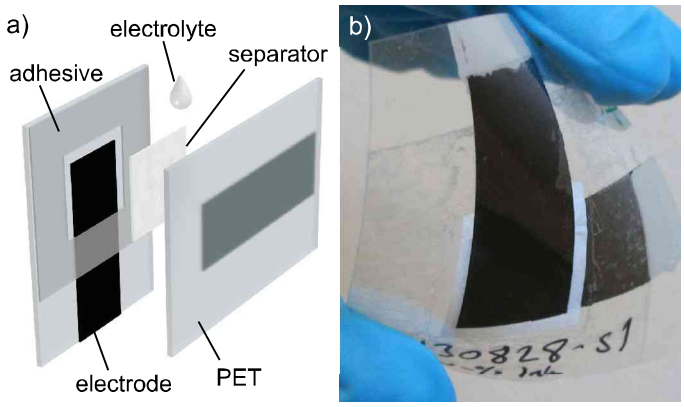

Figure 1: (a) The structure of the assembled supercapacitor. (b) A photograph of a supercapacitor sample.

of the electrode was studied with FESEM; the electrode was cut and glued on the aluminum pin stub followed by carbon-coating to avoid charging of the insulating substrate.

The MWNT ink was stirred before the coating process. A Scotch tape mask (approximately 100 μm thick) was used to define an electrode area of 1.4 cm by 3.2 cm. The ink was coated manually with a metal doctor blade and 5 to 7 layers were deposited on the same electrode, drying the layers between depositions at 50 °C. Sheet resistances of the electrodes were measured with a Zahner Zennium Electrochemical Workstation with a 4-probe setup [18].

Supercapacitors were assembled by placing a separator paper (NKK TF4050) on the bottom electrode, dropping an excess amount of the electrolyte (1.0 M NaCl in water) on it, and pressing another electrode on top while making sure air bubbles did not get trapped between the layers. The supercapacitor was sealed with an adhesive film (UPM Raflatac). The active area of the device was defined by the electrode overlap, 2 cm^2. The structure of the sample is depicted in Fig. 1a, and a photograph is presented in Fig. 1b.

Electrical measurements of the devices were conducted with the Zahner Zennium. For the electrical characterization, silver flake paste was added to the electrode ends to ensure good contact with the measurement device. Cyclic voltammetry (CV) curves were measured from 0 V to 0.9 V with voltage sweep rates from 5 mV/s to 100 mV/s. The working voltage was selected slightly below the theoretical maximum voltage in aqueous electrolyte in order to minimize unwanted electrochemical reactions which can contribute to leakage.

The capacitance and equivalent series resistance (ESR) were determined from galvanostatic discharge measurements according to an international standard [17], Class 3 ("Power"). First, the supercapacitor was charged from 0 V to 0.9 V with a one-minute ramp, then held at 0.9 V for 30 minutes. After this electrification time, the supercapacitor was discharged with a constant current. The capacitance was calculated from the voltage decline rate between 80 % and 40 % of 0.9 V through $C = -I/(\mathrm{d}V/\mathrm{d}t)$. The leakage current of the supercapacitor at 0.9 V was obtained from the same measurement at the end of the electrification phase.

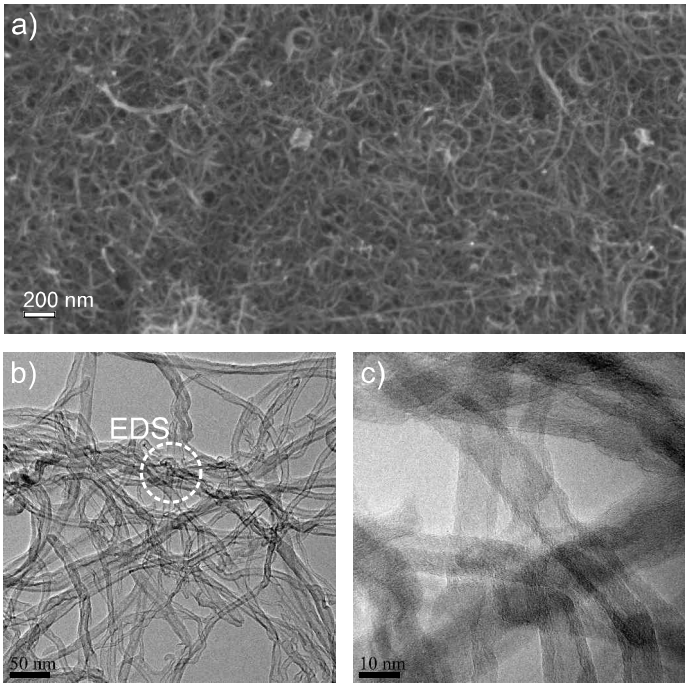

Figure 2: (a) SEM image of the dried MWNT ink, scale bar 200 nm. (b) & (c) TEM images of the dried ink with different magnifications, scale bars 50 nm and 10 nm, respectively.

The discharge current magnitude is defined in the standard with a linear dependence on capacitance, so a short iteration of measurements was also needed for each sample in order to find the right discharge current (typically two iteration steps). The discharge currents used were approximately 50 μA or 10 mA/g. The standard class selection determines the exact current dependence on capacitance: Class 3 is a compromise between the higher A/g values used in most supercapacitor literature and the even lower current used in the standard Class 2 ("Energy storage"). The ESR was determined from the initial IR drop at the start of the discharge phase. The ESR measurement current was 10 times that of the current for the capacitance measurement [17].

Overall ten supercapacitor samples were prepared and characterized. The measurements were conducted directly after assembling the supercapacitors. For three samples, the measurements were also repeated after 3 weeks to assess the aging of the devices.

To further investigate the effect of the class and thus discharge current selection on the capacitance results, the capacitances of three samples were also measured with 10 times lower current and 10 times higher current, corresponding to standard classes 2 and 4. Additionally, the current dependence of the results was simulated with a PSpice circuit simulation software (Cadence OrCAD Capture) using a simple RC model as an equivalent circuit for the supercapacitor.

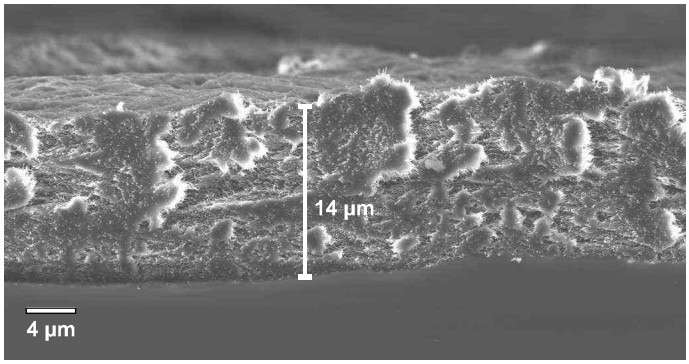

Figure 3: SEM image of the electrode cross section.

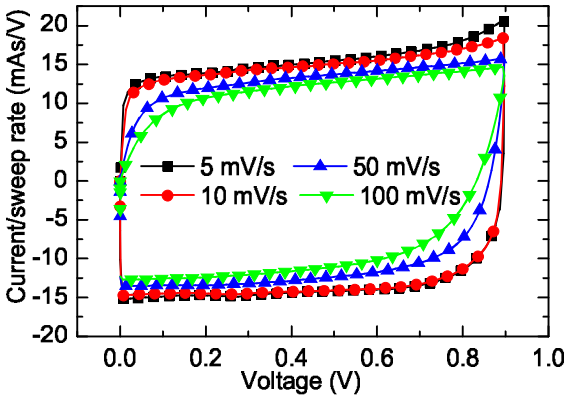

Figure 4: Normalized CV curves at different voltage sweep rates.

3. Results and discussion

SEM and TEM images of the MWNT ink are presented in Fig. 2. The nanotubes are well dispersed and form a random network. EDS analysis of the area marked in Fig. 2b indicates elemental composition of under 1 wt-% impurities such as Na and Fe. This reflects the high purity level of the CNT nanocomposite material [19]. In supercapacitors, a low impurity content of the electrodes is important, as the impurities can go through electrochemical reactions and thus contribute to leakage.

A SEM image of the electrode cross section is presented in Fig. 3. The cross-section image reveals the roughness of the electrode layer: the thickness varies between 13 and 16 µm. Aggregated areas of nanotubes can be seen, as well as large open pores (several µm) leading to deeper in the electrode. These larger pores increase the available surface area, but as there is no separate current collector, they may also inhibit the lateral current flow in the electrode, increasing the ESR.

CV was performed to get a qualitative view of device properties, as it is not recommended as a quantitative method [16]. The CV curves normalized to the different voltage sweep rates are presented in Fig. 4. The box-like shape of the curves indicates good capacitive behavior. Furthermore, the curve retains its shape quite well even at the high voltage sweep rate of 100 mV/s, which indicates quick charge propagation in the double layer capacitance formation [20].

The 5 mV/s and 10 mV/s curves have lower normalized currents than the higher sweep rate curves; ideally, the current divided with sweep rate should stay constant. This is for the most part caused by the series resistance, but the migration time of the electrolyte ions deep into the pores plays a role as well: with a fast sweep rate, only the outermost surface area of the pores is effectively available.

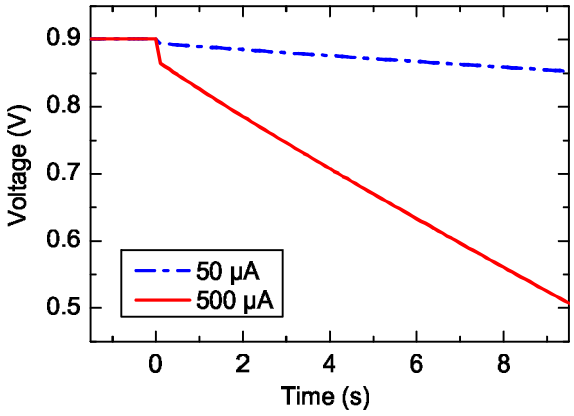

Figure 5: Typical galvanostatic discharge curves. The capacitance is determined from the slope of the lower current discharge (dashed line) and the ESR from the IR drop of the voltage in the beginning of the higher current discharge (solid line).

The capacitance and ESR of the devices were determined from the galvanostatic discharge curves shown in Fig. 5. The capacitance of the devices was on average 12 mF, but due to different layer thicknesses, the capacitances varied between devices, from 10 mF to 15 mF. The leakage current of the supercapacitors was on average 7 µA.

The specific capacitance of the devices was on average 2.3 F/g, calculated from the device capacitance and total electrode mass on the overlapping electrode areas. This corresponds [16] to an electrode specific capacitance of 9.2 F/g. The interpretation of the specific capacitance is not straightforward in CNT supercapacitors without a current collector, as the bottom of the electrode may not contribute much to the double layer capacitance, but is still needed for sufficient conductivity. This is important to note when comparing the specific capacitance to that of supercapacitor materials tested in conventional cells.

The large amount of xylan in the ink forms a layer on the nanotubes, facilitating their dispersion in water. However, it may also lower the double layer capacitance on the surface of the nanotubes by increasing the effective distance between the electrolyte ions and the charged electrode. For this reason, the capacitance is somewhat lower than in previous results of CNT supercapacitors, such as 9.9 mF for a 1 cm^2 supercapacitor by Hu et al. [14]. Here, however, the concentration of the CNT ink was an order of magnitude larger.

As there was no current collector, the average ESR was relatively large, 80 Ω, which is of similar magnitude with previous studies of CNT supercapacitors without a current collector [6, 15]. The sheet resistance of the electrodes was on average 15 Ω/□, a large value compared to metallic current collectors in commercial devices, which have sheet resistances below 0.1 Ω/□ [15]. The lower conductivity of the CNT layer is there-

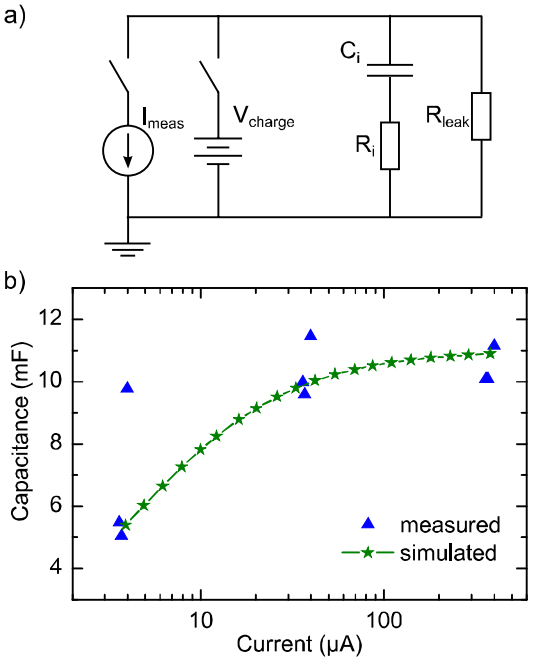

Figure 6: a) The simulation circuit of the galvanostatic measurement; V_{charge} = 0.9 V, C_i = 11 mF, R_i = 100Ω and R_L = 130kΩ. The component values were chosen such that the obtained supercapacitor properties were similar to measured values. The charging voltage is applied for 30 min, after which the circuit is switched to discharge by the constant current source. b) Capacitance results from the simulated and measured discharge curves at different discharge currents.

fore the main cause for the large ESR, although the electrolyte contributes to it as well. Applying a thicker layer of the MWNT ink can therefore reduce the ESR.

The effect of the galvanostatic measurement current on the obtained capacitance value was investigated with an RC circuit model depicted in Fig. 6(a), where the component values were selected to roughly fit the experimental results. The 130 kΩ leakage resistance for the model was obtained from the measured leakage current at 0.9 V. The capacitances were calculated from the simulated discharge curves. The results are shown in Fig. 6(b) with measured capacitances from three samples.

The capacitance decreases with decreasing discharge current, although the variation between samples is relatively large. The main reason for the decrease is the leakage current, which discharges the capacitor at the same time as the external discharge circuit, leading to a faster fall in voltage and thus a smaller apparent capacitance. The effect of the leakage on the results from a slow galvanostatic discharge measurement is important to note when choosing the measurement current in this method. Another factor effecting the galvanostatic discharge results is of course the varying effective time constant of the electrodes, originating from different ion migration times to the bottoms of electrode pores. This can be modeled by adding parallel RC branches to the equivalent circuit [21]. Slower RC branches should lead to a increasing observed capacitance in a galvanostatic discharge experiment with decreasing current. In this case however, the leakage current is large enough to mask such effects.

Samples measured three weeks after assembly displayed an increase of approximately 20 % in capacitance. The increase may be the result of a slow wetting of the electrode. As can be seen in Fig. 3, there are areas in the electrode where the material is quite tightly packed, which could lead to the slow wetting. When the measurements were performed with freshly assembled supercapacitors, all of the available electrode surface area may not have been in contact with the electrolyte.

4. Conclusions

Supercapacitors were prepared on a plastic substrate with a high-viscosity, concentrated carbon nanotube ink. The ink is a mass-production-ready material and it has already been used in industrial scale trials of other products. Future goals for development are to enhance printability on a wider variety of materials and to improve the conductivity of the coating in supercapacitor applications. There is a trade-off between the printability and electrode material quality, the optimization of which is also essential.

The obtained capacitance was on average 12 mF for 2 cm^2 devices. Using aqueous NaCl as the electrolyte makes the devices environmentally friendly and safe, which can in some cases be more important than the higher operating voltage obtained with flammable and harmful organic electrolytes. The scalable single-step solution-processed electrode fabrication enables the integration of supercapacitors to a wide range of applications in printed elecronic circuits.

5. Acknowledgement

The authors thank Veijo Kangas of Morphona for the preparation of the ink. The authors acknowledge funding from the Academy of Finland (Dec. No. 138146 and 139881) and the Finnish Funding Agency for Technology and Innovation (TEKES, Dec. No. 40049/12). S. Lehtimäki would like to thank Tekniikan edistämissäätiö for supporting the research.

References

[1] Kötz R, Carlen M. Principles and applications of electrochemical capacitors. Electrochim Acta 2000;45(15-16):2483–98. doi:10.1016/S0013-4686(00)00354-6.

[2] Frackowiak E, Béguin F. Carbon materials for the electrochemical storage of energy in capacitors. Carbon 2001;39(6):937–50. doi:10.1016/S0008-6223(00)00183-4.

[3] Pandolfo AG, Hollenkamp AF. Carbon properties and their role in supercapacitors. J Power Sources 2006;157(1):11–27. doi:10.1016/j.jpowsour.2006.02.065.

[4] Simon P, Gogotsi Y. Materials for electrochemical capacitors. Nat Mater 2008;7(11):845–54. doi:10.1038/nmat2297.

[5] Keskinen J, Sivonen E, Jussila S, Bergelin M, Johansson M, Vaari A, et al. Printed supercapacitors on paperboard substrate. Electrochim Acta 2012;85:302–6. doi:10.1016/j.electacta.2012.08.076.

[6] Kaempgen M, Chan CK, Ma J, Cui Y, Gruner G. Printable thin film supercapacitors using single-walled carbon nanotubes. Nano Lett 2009;9(5):1872–6. doi:10.1021/nl8038579.

[7] Somov A, Ho CC, Passerone R, Evans JW, Wright PK. Towards extending sensor node lifetime with printed supercapacitors. In: Picco GP, Heinzelman W, editors. Wireless Sensor Networks, Proceedings of the 9th European Conference, EWSN 2012, Trento, Italy, February 15-17, 2012. Springer; 2012, p. 212–27. doi:10.1007/978-3-642-28169-3_14.

[8] Simjee F, Chou PH. Everlast: long-life, supercapacitor-operated wireless sensor node. In: Low Power Electronics and Design, 2006. ISLPED'06. Proceedings of the 2006 International Symposium on. IEEE; 2006, p. 197–202. doi:10.1109/LPE.2006.4271835.

[9] Lehtimäki S, Li M, Salomaa J, Pörhönen J, Kalanti A, Tuukkanen S, et al. Performance of printable supercapacitors in an RF harvesting circuit. 2014. (Accepted for publication in International Journal of Electrical Power & Energy Systems).

[10] Kaempgen M, Ma J, Gruner G, Wee G, Mhaisalkar SG. Bifunctional carbon nanotube networks for supercapacitors. Appl Phys Lett 2007;90(26):264104. doi:10.1063/1.2749187.

[11] Tuukkanen S, Julin T, Rantanen V, Zakrzewski M, Moilanen P, Lilja KE, et al. Solution-processible electrode materials for a heat-sensitive piezoelectric thin-film sensor. Synthetic Met 2012;162(21):1987–95. doi:10.1016/j.synthmet.2012.08.021.

[12] Kim SW, Kim T, Kim YS, Choi HS, Lim HJ, Yang SJ, et al. Surface modifications for the effective dispersion of carbon nanotubes in solvents and polymers. Carbon 2012;50(1):3–33. doi:10.1016/j.carbon.2011.08.011.

[13] Hu L, Choi JW, Yang Y, Jeong S, La Mantia F, Cui LF, et al. Highly conductive paper for energy-storage devices. P Natl Acad Sci 2009;106(51):21490–4. doi:10.1073/pnas.0908858106.

[14] Hu L, Wu H, Cui Y. Printed energy storage devices by integration of electrodes and separators into single sheets of paper. Appl Phys Lett 2010;96(18):183502–. doi:10.1063/1.3425767.

[15] Hu S, Rajamani R, Yu X. Flexible solid-state paper based carbon nanotube supercapacitor. Appl Phys Lett 2012;100(10):104103. doi:10.1063/1.3691948.

[16] Stoller MD, Ruoff RS. Best practice methods for determining an electrode material's performance for ultracapacitors. Energy Environ Sci 2010;3(9):1294–301. doi:10.1039/C0EE00074D.

[17] International Electrotechnical Comission . International standard: Fixed electric double layer capacitors for use in electronic equipment, IEC 62391-1. 2006.

[18] Smits FM. Measurement of sheet resistivities with the four-point probe. Bell Syst Tech J 1958;37(3):711–18.

[19] Li Y, Zhang X, Tao X, Xu J, Huang W, Luo J, et al. Mass production of high-quality multi-walled carbon nanotube bundles on a Ni/Mo/MgO catalyst. Carbon 2005;43(2):295–301.

[20] Xu Y, Lin Z, Huang X, Wang Y, Huang Y, Duan X. Functionalized graphene hydrogel-based high-performance supercapacitors. Adv Mater 2013;25(40):5779–84. doi:10.1002/adma.201301928.

[21] Zubieta L, Bonert R. Characterization of double-layer capacitors for power electronics applications. Industry Applications, IEEE Transactions on 2000;36(1):199–205. doi:10.1109/28.821816.